J. Fluid Mech. (2010), *vol.* 642, *pp.* 127–146. © Cambridge University Press 2010
doi:10.1017/S0022112009991716

Maximum intensity of rarefaction shock waves for dense gases

ALBERTO GUARDONE[1], CALIN ZAMFIRESCU[2] AND PIERO COLONNA[3]†

[1]Dipartimento di Ingegneria Aerospaziale, Politecnico di Milano Via La Masa 34, Milano 20156, Italy

[2]Faculty of Engineering and Applied Science, University of Ontario Institute of Technology, 2000 Simcoe Street North, Oshawa, ON L1H 74K, Canada

[3]Process and Energy Department, Delft University of Technology Leghwaterstraat 44, Delft, 2628 CA, The Netherlands

(Received 12 December 2008; revised 14 August 2009; accepted 15 August 2009)

Modern thermodynamic models indicate that fluids consisting of complex molecules may display non-classical gasdynamic phenomena such as rarefaction shock waves (RSWs) in the vapour phase. Since the thermodynamic region in which non-classical phenomena are physically admissible is finite in terms of pressure, density and temperature intervals, the intensity of RSWs is expected to exhibit a maximum for any given fluid. The identification of the operating conditions leading to the RSW with maximum intensity is of paramount importance for the experimental verification of the existence of non-classical phenomena in the vapour phase and for technical applications taking advantage of the peculiarities of the non-classical regime. This study investigates the conditions resulting in an RSW with maximum intensity in terms of pressure jump, wave Mach number and shock strength. The upstream state of the RSW with maximum pressure drop is found to be located along the double-sonic locus formed by the thermodynamic states associated with an RSW having both pre- and post-shock sonic conditions. Correspondingly, the maximum-Mach thermodynamic and maximum-strength loci locate the pre-shock states from which the RSW with the maximum wave Mach number and shock strength can originate. The qualitative results obtained with the simple van der Waals model are confirmed with the more complex Stryjek–Vera–Peng–Robinson, Martin–Hou and Span–Wagner equations of state for selected siloxane and perfluorocarbon fluids. Among siloxanes, which are arguably the best fluids for experiments aimed at the generation and measurement of an RSW, the state-of-the-art Span–Wagner multi-parameter equation of state predicts a maximum wave Mach number close to 1.026 for D_6 (dodecamethylcyclohexasiloxane, $[O\text{-}Si\text{-}(CH_3)_2]_6$). Such value is well within the capacity of the measurement system of a newly built experimental set-up aimed at the first-ever demonstration of the existence of RSWs in dense vapours.

Key words: gas dynamics, shock waves

1. Introduction

The existence of so-called non-classical gasdynamic phenomena in the single-phase vapour region is still an open question of fluid mechanics. This kind of 'exotic'

† Email address for correspondence: P.Colonna@TUDelft.nl

gasdynamic specimens, which include rarefaction shock waves (RSWs) and mixed or split waves (see Menikoff & Plohr 1989), have been observed experimentally in flows displaying liquid–vapour phase transition by Thompson, Carofano & Kim (1986); see also Thompson *et al.* (1987) and by Ivanov & Novikov (1961) in allotropic phase changes in steel. Starting from the pioneering works of Bethe (1942), Zel'dovich (1946), Weyl (1949) and Thompson (1971), the possibility of observing non-classical gasdynamic phenomena also in the dense-vapour region has been investigated in numerous theoretical and numerical studies. Indeed, modern thermodynamic models indicate that a bounded thermodynamic region in the vapour phase where non-classical gasdynamic phenomena are physically admissible may exist for a class of fluids – named Bethe–Zel'dovich–Thompson (BZT) fluids – characterized by high molecular complexity. According to predictions from several thermodynamic models reported by Thompson & Lambrakis (1973), Cramer (1991), Colonna & Silva (2003), Guardone & Argrow (2005), Colonna, Guardone & Nannan (2007) and others, heavy hydrocarbons, perfluorocarbons and siloxanes can be classified as BZT fluids.

Despite the large amount of available theoretical and numerical studies on non-classical gasdynamics, a limited amount of experimental work has been performed so far, mainly due to the technical difficulties related to the observation of these kind of waves, as discussed by Fergason, Guardone & Argrow (2003) and Colonna *et al.* (2008*a*). A first attempt at measuring an RSW in Freon-13 (trifluorochloromethane, CCl_3F) has been carried out in the USSR by Borisov *et al.* (1983). Indeed, a rarefaction wave propagating with a steady profile was measured, but recent interpretations of that experiment explain the occurrence of such a wave as a result of critical-point and two-phase effects, as discussed by Cramer & Sen (1986), Kutateladze, Nakoryakov & Borisov (1987), Thompson (1991), Fergason *et al.* (2001), Fergason, Guardone & Argrow (2003) and Nannan (2009). More recently, a shock-tube experiment, documented by Fergason *et al.* (2003) and Guardone (2007), has been pursued at the University of Colorado at Boulder, with the aim of producing an RSW in perfluorocarbon fluid PP10 (Perfluorofluorene, $C_{13}F_{22}$). The non-classical character of the rarefaction wave was to be determined by comparing the wave velocity, measured by a simple time-of-flight approach, with the estimate of the speed of sound in the unperturbed state; an RSW moves at supersonic speed, while a classical rarefaction wave moves at the speed of sound. The Boulder experiment eventually failed because the working fluid underwent thermal decomposition at the extremely high operating temperature. In addition the lack of accurate information on the thermophysical properties of the working fluid would have prevented the estimation of the speed of sound with the accuracy needed to claim that the observed wave was indeed supersonic.

Building on the experience acquired during the Boulder experiment, a novel set-up for the generation of RSWs has been conceived, designed and constructed at the Delft University of Technology, the Netherlands, with the participation of the Politecnico di Milano, Italy (see Colonna *et al.* 2008*a*). The flexible asymmetric shock tube (FAST) set-up is a dense gas Ludwieg tube, made of a high-pressure charge tube connected to a low-pressure reservoir. The charge tube and the reservoir are separated by a fast-opening valve. The fluid is initially at rest, and its temperature is kept uniform by a suitable thermal control system. The experiment starts when the valve is opened, thus connecting the charge tube to the reservoir. An RSW is expected to form and propagate towards the end of the charge tube, where pressure transducers measure the wave speed by means of a time-of-flight approach. The speed of the rarefaction front is compared to the local value of the speed of sound to determine if the propagating wave is a shock moving at supersonic speed. The speed of sound in the unperturbed

state is accurately measured in a similar way prior to the experiment, by producing small (acoustic) pressure waves propagating along the charge tube, thus eliminating the need of computing the value of the speed of sound by means of a thermodynamic model, whose accuracy in the region of interest is questionable. The working fluid selected for the experiment is siloxane fluid D_6 (dodecamethylcyclohexasiloxane, $[O\text{-}Si\text{-}(CH_3)_2]_6$). Comparably accurate thermodynamic models for siloxanes have been recently developed (see Colonna *et al.* 2006; Colonna, Nannan & Guardone 2008*b*), and they also rely on precise speed-of-sound measurements and molecular simulations (see Nannan *et al.* 2007). Moreover, the thermal stability limit of siloxanes in stainless steel has been experimentally investigated by Angelino & Invernizzi (1993) and Colonna (1996), and suitable procedures to avoid or delay the thermal decompositions of the working fluid have been devised (see Calderazzi & Colonna 1997). Despite the mentioned improvements, the determination of the non-classical character of the wave remains a difficult endeavour, as discussed by Colonna *et al.* (2008*a*).

Fergason *et al.* (2001) observed that experimental constraints can be significantly relaxed by producing a strong RSW. For example, by maximizing the wave Mach number – the ratio of the wave speed to the speed of sound in the still fluid – the requirements on the accuracy for the determination of both the wave speed and the local value of the speed of sound are minimized. Accordingly, Fergason *et al.* (2001) derived an empirical procedure to determine the initial shock-tube states that would result in the largest pressure difference across the wave, with the understanding that such an RSW would also exhibit a large Mach number.

This study moves from a previous work by Zamfirescu, Guardone & Colonna (2008), and it is focused on the determination of the states which generate the RSW with the largest intensity for a given BZT fluid. An analytical procedure is derived to identify the thermodynamic states resulting in the RSW exhibiting the maximum pressure difference, the RSW with maximum Mach number and the RSW with the largest strength, over the entire dense-vapour thermodynamic region. Note that these conditions are not equivalent and that three different waves are to be computed for each fluid. The identification of these special RSWs is important for both the experimental activities currently under way and the design of machinery to be operated in the non-classical regime. A notable example of a possible industrial application is the organic Rankine cycle turbine, in which non-classical phenomena could be induced in order to reduce losses due to the occurrence of classical compression shock waves (see Brown & Argrow 2000) or due to boundary-layer separation following the interaction of a compression shock with the boundary layer (see Cramer & Park 1999).

The structure of the paper is as follows. In § 2, relevant results on RSWs are briefly recalled. Section 3 details a procedure to determine the RSW with maximum pressure jump, wave Mach number and strength for a given fluid, using the simple van der Waals (1873) model. In § 4, accurate multi-parameter models are used to compute the RSW with maximum intensity for selected siloxanes and perfluorocarbons. Section 5 presents final remarks and comments.

2. Rarefaction shock waves (RSWs) in dense gases

For the sake of clarity, relevant results on the theory of RSWs are briefly recalled here, starting from the definition of the fundamental derivative of gasdynamics,

$$\Gamma \equiv \frac{v^3}{2c^2}\left(\frac{\partial^2 P}{\partial v^2}\right)_s = 1 - \frac{v}{c}\left(\frac{\partial c}{\partial v}\right)_s, \tag{2.1}$$

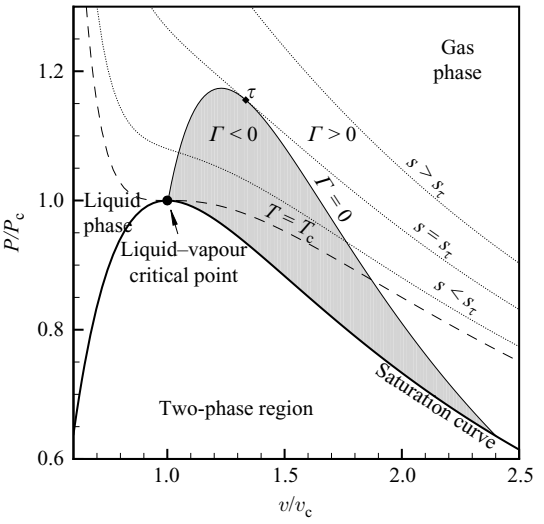

FIGURE 1. Liquid–vapour saturation curve (—) and the $\Gamma < 0$ region (shaded region) for a BZT fluid in the volume–pressure plane computed from the polytropic van der Waals model with $N = 2000$. Selected isentropes $(\cdots)$ and the critical isotherm $T = T_c$ $(- \ -)$ are also indicated. Note that the isentropes are concave down in the $\Gamma < 0$ region. The isentrope s_τ is tangent to the $\Gamma = 0$ line in τ.

where v is the specific volume; P is the pressure; and $c \equiv -v(\partial P/\partial v)_s^{1/2}$ is the speed of sound. The subscript s indicates that the pressure derivative is computed at constant entropy. The fundamental derivative of gasdynamics was introduced by Thompson (1971) to identify thermodynamic states possibly leading to non-classical behaviour, which is heralded by negative values of Γ. Indeed, Bethe (1942) and Weyl (1949) independently showed that an RSW is physically admissible if it connects two states within the $\Gamma < 0$ region, due to the negative curvature of the isentropes – and hence of the shock adiabats – in this region. As is well known, for a polytropic (constant isochoric heat capacity) ideal gas both the isentropes and the shock adiabats are always concave up and RSWs are not thermodynamically admissible.

According to the polytropic van der Waals model, fluids with large molecular complexity exhibit a $\Gamma < 0$ region in the dense-vapour phase, close to the liquid–vapour equilibrium line and close to the critical point. The size of this region increases with increasing molecular complexity, which, for a polytropic van der Waals gas, depends only on the (constant) number of active degrees of freedom of the molecule N (see Colonna & Guardone 2006). For the temperatures of interest here, these include the translational, rotational and vibrational modes only. From the energy equipartition principle (see Callen 1985), one has $N = 2c_v/R$, with c_v (constant) isochoric specific heat and $R = \mathscr{R}/M$, with $\mathscr{R} = 8.314$ J mol^{-1} the universal gas constant and M the molecular weight. The existence of a $\Gamma < 0$ region in the vapour phase and its dependence on molecular complexity is confirmed also by more complex thermodynamic models (see for example Thompson & Lambrakis 1973; Cramer 1991; Colonna & Silva 2003; Colonna *et al.* 2007, under review), although the location and size of the $\Gamma < 0$ region strongly depends on the considered thermodynamic model (see Guardone & Argrow 2005; Colonna *et al.*, under review). Figure 1 shows representative isentropes close to the liquid-saturation curve, together with the critical isotherm $T = T_c$ and the $\Gamma < 0$ region, for a polytropic van der Waals

gas with $N = 2000$. This value of N is unrealistically high, and it is considered here only for explanatory purposes.

Remarkably enough, the occurrence of RSWs is not limited to state points within the $\Gamma < 0$ region. Thompson & Lambrakis (1973) were the first researchers who observed that an RSW can possibly occur also between two states with $\Gamma > 0$, provided that the supporting Rankine–Hugoniot curve crosses the $\Gamma < 0$ region. With reference to figure 1, note that an RSW cannot originate from any state with $s > s_\tau$, where s_τ is the entropy associated with the isentrope that is tangent to the $\Gamma = 0$ curve. This is due to the fact that the post-shock entropy is always larger than the pre-shock one, and therefore shock adiabats starting from a state with $s > s_\tau$ do not cross the $\Gamma < 0$ region.

To identify all possible flow conditions leading to the formation of an RSW, including those connecting thermodynamic states with $\Gamma > 0$, some basic properties of RSWs are briefly illustrated. As is well known, all flow discontinuities, including RSWs, satisfy the Rankine–Hugoniot relations between the two states A and B separated by the shock (see e.g. Hayes 1960),

$$\left.\begin{aligned} u_A/v_A &= u_B/v_B, \\ P_A + u_A^2/v_A &= P_B + u_B^2/v_B, \\ h(P_A, v_A) + \frac{1}{2}u_A^2 &= h(P_B, v_B) + \frac{1}{2}u_B^2, \end{aligned}\right\} \tag{2.2}$$

where the enthalpy h is computed from the pressure and the specific volume via enthalpy-explicit equation of state $h = h(P, v)$. The flow velocity u is evaluated in a reference frame moving at the velocity of the shock. The above system allows one to compute the post-shock state B corresponding to a given pre-shock condition A. By combining the mass, momentum and energy conservation laws in system (2.2), one immediately obtains $h(P_B, v_B) - h(P_A, v_A) - (P_B - P_A)(v_A + v_B)/2 = 0$, which provides the implicit definition of the Rankine–Hugoniot curve or shock adiabat centred at A, i.e.

$$P_B = P^H(v_B, P_A, v_A), \tag{2.3}$$

where P^H is the so-called Hugoniot pressure function. (2.3) allows one to compute the post-shock value of the pressure P_B as a function of the post-shock specific volume v_B for a given pre-shock state A, defined in terms of both the pre-shock pressure and specific volume, P_A and v_A respectively. By combining the conservation of mass and momentum equations in system (2.2), the Rayleigh line is obtained as

$$P_B = P^R(v_B, P_A, v_A, u_A) = P_A + \left(1 - \frac{v_B}{v_A}\right)\frac{u_A^2}{v_A}, \tag{2.4}$$

with P^R the Rayleigh pressure function. Eventually, the downstream specific volume v_B is found by solving for v_B the equation

$$P^H(v_B; P_A, v_A) = P^R(v_B; P_A, v_A, u_A), \tag{2.5}$$

in which the pre-shock values of the pressure, specific volume and velocity are known. By substituting the value of v_B from (2.5) into system (2.2) the remaining post-shock variables are easily computed.

Zamfirescu *et al.* (2008) proved the existence and the uniqueness of the solution to the shock problem (2.5) for a dense gas using the theorem of Liu (1975) for a general, i.e. non-ideal, gas. The unique admissible downstream state among all possible solutions to (2.5) is selected by imposing the entropy condition $\Delta s > 0$ (see Oleinik

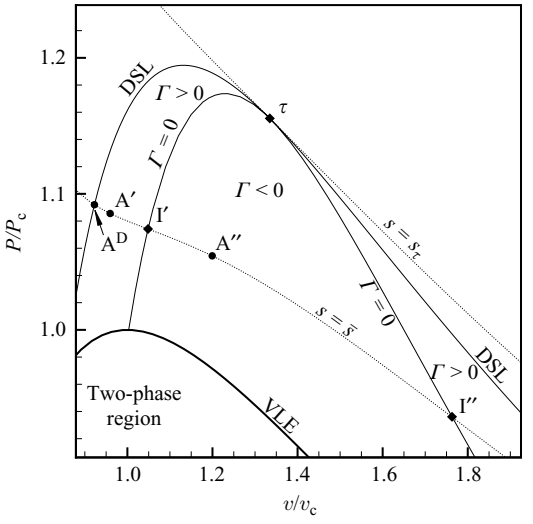

FIGURE 2. Selected pre-shock points A^D, A' and A'' along the isentrope $s = \bar{s} < s_\tau$ for a van der Waals polytropic gas with $N = 2000$. Points I' and I'' are the intersections of $s = \bar{s}$ with the $\Gamma = 0$ curve. The vapour–liquid equilibrium (VLE) line is drawn together with the double-sonic locus (DSL).

1959; Smoller 1983), which, together with the shock stability or speed orienting condition $M_A \geqslant 1 \geqslant M_B$, with $M = |u|/c$ the Mach number (see Lax 1957), gives

$$\frac{\mathrm{d}P^{\mathrm{H}}}{\mathrm{d}v_{\mathrm{B}}}\Big|_A \geqslant \frac{\mathrm{d}P^{\mathrm{R}}}{\mathrm{d}v_{\mathrm{B}}}\Big|_A \equiv \frac{P_{\mathrm{A}} - P_{\mathrm{B}}}{v_{\mathrm{A}} - v_{\mathrm{B}}} \equiv \frac{\mathrm{d}P^{\mathrm{R}}}{\mathrm{d}v_{\mathrm{B}}}\Big|_B \geqslant \frac{\mathrm{d}P^{\mathrm{H}}}{\mathrm{d}v_{\mathrm{B}}}\Big|_B, \tag{2.6}$$

where equalities hold for sonic pre- or post-shock states (see Kluwick 2001). Note that neither pre-shock sonic nor post-shock sonic shocks are admissible for ideal polytropic gases. Criterion (2.6) provides a simple geometrical condition for the admissibility of rarefaction shock waves in dense gases. According to (2.6), the (constant) slope of the Rayleigh line in the v–P plane must be smaller than that of the tangent to the shock adiabats in A and larger than that at the post-shock state B. Consequently, for an RSW to be admissible the shock adiabat necessarily exhibits downward concavity, at least in a limited portion of the shock adiabat itself; admissible shock waves are such that the associated Rayleigh line lies completely below the shock adiabat (see Cramer & Sen 1990).

Scenarios for the formation of an RSW in a BZT vapour are treated extensively in Menikoff & Plohr (1989), Kluwick (2001) and Zamfirescu *et al.* (2008). Relevant results are briefly recalled here with the help of figures 2 and 3. Figure 2 shows a portion of the specific volume–pressure thermodynamic plane for a BZT fluid in which selected pre-shock state points A^D, A' and A'' along one and the same isentrope $s = \bar{s} < s_\tau$ are indicated. All isentropes with $s < s_\tau$ exhibit the same qualitative shape, with two inflection points at the intersections I′ and I″ with the $\Gamma = 0$ curve. Possible cases for the formation of an RSW can be inspected in figure 3, where the shock adiabats and the isentropes through the pre-shock state are plotted for selected pre-shock state points A^D, A' and A'' together with representative Rayleigh lines and post-shock states corresponding to admissible RSWs. Note that all Rayleigh lines lie below the shock adiabats, and therefore the associated RSWs satisfy the admissibility condition (2.6). Figure 3(*a*) corresponds to a quite peculiar situation in which the

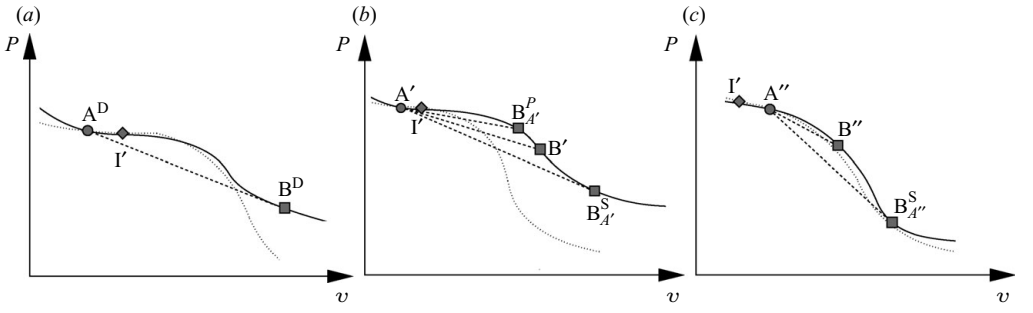

FIGURE 3. Shock adiabat from the pre-shock state A (—) and Rayleigh line A–B (- - -) for different initial pre-shock states along an isentrope crossing the $\Gamma < 0$ region in the vapour phase. (*a*) From point $A^{\mathrm{D}}(\bar{s})$, only a double-sonic RSW A^{D}–B^{D} is admissible, where $B^{\mathrm{D}} = B^{\mathrm{D}}(\bar{s})$. (*b*) From point A', located in the $\Gamma > 0$ region in between the DSL and the $\Gamma = 0$ curve, possible RSWs include the pre-shock sonic RSW A'–$B^{P}_{A'}$ and the post-shock sonic RSW A'–$B^{\mathrm{S}}_{A'}$. All shocks connecting A' to state points in between $B^{P}_{A'}$ and $B^{\mathrm{S}}_{A'}$, such as A'–B', are admissible and are neither pre- nor post-shock sonic. (*c*) From A'', which lies within the $\Gamma < 0$ region, no pre-shock sonic RSWs are admissible. The post-shock sonic RSW A''–$B^{\mathrm{S}}_{A''}$ is admissible, as well as all non-sonic shock connecting A'' to state points in between A'' and $B^{\mathrm{S}}_{A''}$, such as A''–B''.

only admissible RSW is a double-sonic shock, namely a shock in which both the pre-shock Mach number $M_{A^{\mathrm{D}}}$ and the post-shock Mach number $M_{B^{\mathrm{D}}}$ are unity (see Thompson & Lambrakis 1973; Cramer & Sen 1990). The Rayleigh line is tangent to the shock adiabat from A^{D} at both the pre-shock state and the post-shock state B^{D}. Similar to an acoustic wave, a double-sonic RSW moves at sonic speed, but different from the former, through the RSW a finite jump in the thermodynamic properties of the fluid and in its local velocity occurs. As demonstrated by Zamfirescu *et al.* (2008), along each isentrope only one double-sonic RSW is admissible. By varying the value of the pre-shock entropy, one can draw the double-sonic locus (DSL) of the pre-shock states $A^{\mathrm{D}} = A^{\mathrm{D}}(s)$ and the post-shock states $B^{\mathrm{D}} = B^{\mathrm{D}}(s)$ which can be connected by a double-sonic RSW. Note that $s_{B^{\mathrm{D}}} \neq s_{A^{\mathrm{D}}}$. The $\Gamma < 0$ region lies within the DSL and the VLE; no RSW can originate from state points outside the DSL, which is indicated by Zamfirescu *et al.* (2008) as the boundary of the rarefaction shock region (RSR) comprising all state points that can be connected by an RSW (see figure 4*b*). Figure 3(*b*) shows admissible RSWs for pre-shock states located in between the DSL and the $\Gamma = 0$ curve, on the left of the $\Gamma < 0$ region in figure 2. These are the pre-shock sonic ($M_{A'} = 1$) RSW A'–$B^{P}_{A'}$, the post-shock sonic ($M_{B^{\mathrm{S}}} = 1$) RSW A'–$B^{\mathrm{S}}_{A'}$ and all non-sonic shocks with post-shock states in between $B^{P}_{A'}$ and $B^{\mathrm{S}}_{A'}$, such as A'–B'. Note that the Rayleigh line is tangent to the shock adiabat from A' at the pre-shock state for the pre-shock sonic shock A'–$B^{P}_{A'}$ and to the post-shock state $B^{\mathrm{S}}_{A'}$ for the post-shock sonic one. No pre-shock sonic RSW can originate from pre-shock states lying within the $\Gamma < 0$ region, e.g. point A'' in figure 3(*c*). Instead, only post-shock sonic RSW such as shock A''–$B^{\mathrm{S}}_{A''}$ are possible, together with non-sonic shocks with post-shock states in between A'' and $B^{\mathrm{S}}_{A''}$, such as A''–B''. Finally, no RSW can originate from state points located in between the $\Gamma = 0$ curve and the DSL, on the right of the $\Gamma < 0$ region, because the rarefactive portion of the shock adiabat is always concave up for all possible pre-shock states.

To each pre-shock state A from which an RSW can possibly originate corresponds one and only one post-shock state B leading to post-shock sonic conditions. This state

can be easily computed by complementing system (2.2) with the additional condition $u_B = c(P_B, v_B)$. The existence and uniqueness of the post-shock sonic state follows immediately from the above discussion and from the uniqueness of the solution of the Riemann problem for dense gases proved by Zamfirescu *et al.* (2008).

In the following, post-shock sonic states are indicated as $B_A^S = B_A^S(s_A, v_A)$, to underline their dependence on the pre-shock state A only and the fact that they correspond to sonic conditions. The same nomenclature is used for all quantities evaluated at B_A^S, such as $M_A^S(s_A, v_A) \equiv 1$. Similarly, for double-sonic states, the pre- and post-shock pressures are indicated as P_A^D and P_B^D, respectively.

3. Maximum intensity of rarefaction shock waves (RSWs)

Here, the pre- and post-shock states resulting in the RSW with maximum intensity are derived. In this context, an RSW has the maximum intensity if some relevant fluid properties display maximal variation across it. The properties of interest are the wave Mach number, the pressure variation across the wave and the shock strength. As stated in § 1 the supersonic wave Mach number is arguably the quantity that can be more easily detected in an experiment aimed at demonstrating the existence of RSWs. The pressure difference and the shock strength, providing a measure of the pressure perturbations in relation to the flow velocity, are relevant to possible process applications. Variations involving the temperature are less important, as the temperature does not change much in the studied phenomenon due to the high specific heat of BZT fluids.

As recalled in the previous section, the post-shock state along a given Rankine–Hugoniot curve is completely determined by selecting the value of a single post-shock quantity, e.g. the post-shock specific volume v_B. The definition of the Rankine–Hugoniot curve itself depends instead on two thermodynamic variables at state A, such as the pre-shock specific volume v_A and the pressure P_A. It follows that the determination of the RSW with maximum intensity is a three-dimensional maximization problem for P_A, v_A and v_B over the entire RSW region. It is however possible to reduce the order of the maximization problem by recalling the RSW properties reported in the previous section. This is done in § 3.1 to determine the RSW with maximum pressure difference $\widehat{\Delta P}$, in § 3.2 for the RSW with maximum wave Mach number and in § 3.3 for the RSW with maximum shock strength. For simplicity, all the results presented in this section have been obtained from the van der Waals (1873) model. Section 4 shows that the same results can be obtained with more complex and realistic thermodynamic models.

3.1. *Maximum pressure difference*

Herein, the pre- and post-shock states defining the RSW supporting the largest pressure difference $\widehat{\Delta P}$, with

$$\widehat{\Delta P} = \max_{s_A, v_A, v_B} \left[P^H(s_A, v_A, v_B) - P(s_A, v_A) \right],$$

are determined. Note that both the pre- and post-shock states A and B lie within the RSW region. From the Rankine–Hugoniot system (2.2) one immediately has

$$-(u_A/v_A)^2 = \Delta P/\Delta v = -(u_B/v_B)^2 < 0,$$

with $\Delta P = P_B - P_A$ and $\Delta v = v_B - v_A$. Therefore, $\Delta P < 0$ if $\Delta v > 0$ and the Rankine–Hugoniot curve is a monotonically decreasing function of the post-shock specific

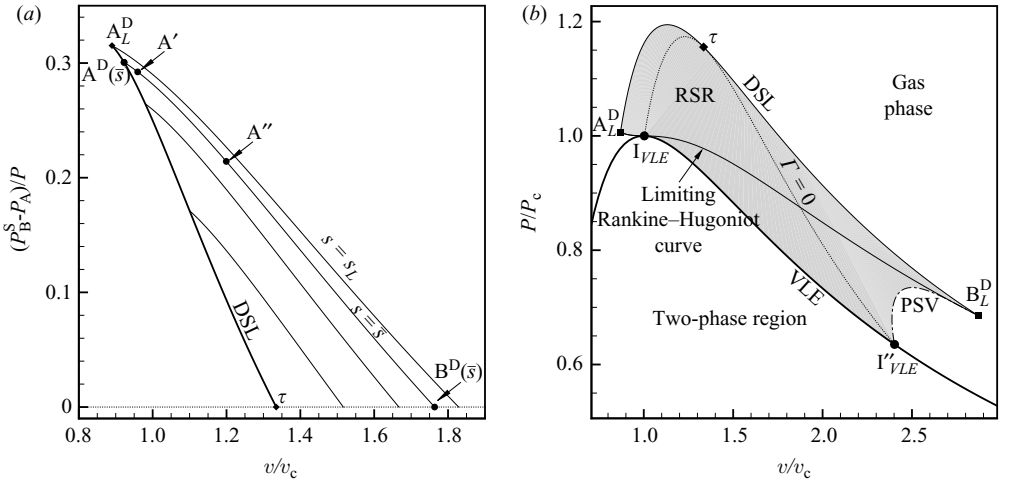

FIGURE 4. (*a*) Reduced pressure difference across post-shock sonic shocks for a polytropic van der Waals fluid with $N = 2000$ along diverse isentropes $s = \text{const.} < s_\tau$. Along a given isentrope, the maximum pressure difference is obtained at the intersection with the DSL, namely for double-sonic shocks A^D–B^D. (*b*) The DSL in the reduced volume–pressure plane v/v_c–P/P_c. The limiting Rankine–Hugoniot curve connects the pre- and post-shock states A_L^D and B_L^D, respectively, of the RSW exhibiting the largest pressure difference. The post-shock sonic from VLE (PSV) line is also drawn, comprising all post-shock point connected to the VLE by a post-shock sonic RSW.

volume (see e.g. Thompson 1988). It follows that the largest pressure difference is observed for a shock wave encompassing the largest difference in specific volumes.

For a given pre-shock state A, the largest pressure difference occurs across the only RSW admitting a downstream sonic point, and the three-dimensional maximization problem simplifies to

$$\widehat{\Delta P} = \max_{s_A, v_A} \left[P_B^S(s_A, v_A) - P(s_A, v_A) \right] = \max_{s_A} \left[P_B^D(s_A) - P_A^D(s_A) \right].$$

Indeed, Δv and hence ΔP are maximal along a given isentrope s_A if state A lies on the DSL line (see figure 4*a*), namely if the RSW is a double-sonic shock.

Furthermore, with reference to figure 4, $\Delta P = \Delta v = 0$ at $s_A = s_\tau$ and ΔP increases monotonically with decreasing entropy. The maximum pressure difference across the shock waves is therefore obtained for the double-sonic shock originating from the state point with the lowest possible entropy $s_A = s_L$. This corresponds to the isentrope through A_L^D; thus

$$\widehat{\Delta P} = P_B^D(s_L) - P_A^D(s_L). \tag{3.1}$$

In figure 4(*b*), the limiting Rankine–Hugoniot curve connecting the pre- and post-shock states A_L^D and B_L^D is drawn, together with the DSL and the PSV line of all post-shock point connected to the VLE by a post-shock sonic RSW. The shaded region is the RSR comprising all state points that can be connected by an RSW.

Thompson & Lambrakis (1973) were the first to identify double-sonic shocks as those exhibiting the largest pressure jump. However, different from the derivation presented here, in their discussion the authors resorted to an isentropic description of the flow.

3.2. *Maximum wave Mach number*

This section is dedicated to the identification of pre- and post-shock states leading to the RSW with maximum wave Mach number. The wave Mach number M_W is defined as the ratio of the wave velocity to the speed of sound in the unperturbed fluid. If the fluid is at rest in the pre-shock state, then the fluid velocity in the shock reference frame is equal to the shock wave velocity in the laboratory frame; hence $M_W \equiv M_A = u_A/c_A$ and from relation (2.4) one immediately obtains

$$[\widehat{M}_W]^2 = -\min_{s_A, v_A, v_B} \left[\frac{v_A}{c(s_A, v_A)}\right]^2 \frac{P^H(s_A, v_A, v_B) - P(s_A, v_A)}{v_B - v_A}. \tag{3.2}$$

Note that a maximum for M_W^2 is also an extremum for M_W. For a given upstream state A, M_W is maximized if $\Delta P/\Delta v$ is minimized, that is if the slope of the Rayleigh line is minimized. The minimum of the slope is obtained at the post-shock sonic state, where the Rayleigh line is tangent to the shock adiabat through A. Therefore, if the post-shock value of the specific volume is chosen as $v_B = v_B^S(s_A, v_A)$, the three-dimensional maximization problem (3.2) reduces to the following two-dimensional one:

$$[\widehat{M}_W]^2 = -\min_{s_A, v_A} \left[\frac{v_A}{c(s_A, v_A)}\right]^2 \frac{P_B^S(s_A, v_A) - P(s_A, v_A)}{v_B^S(s_A, v_A) - v_A}.$$

Since B is sonic, from the definition of the Rayleigh line (2.4) and the shock condition $P^R = P^H$, one also has

$$\frac{P_B^S(s_A, v_A) - P(s_A, v_A)}{v_B^S(s_A, v_A) - v_A} \equiv -\left[\frac{u_B}{v_B}\right]^2 = -\left[\frac{c_B^S(s_A, v_A)}{v_B^S(s_A, v_A)}\right]^2, \tag{3.3}$$

and therefore

$$\widehat{M}_W = \max_{s_A, v_A} M_W^S(s_A, v_A) = \max_{s_A, v_A} \frac{v_A}{c(s_A, v_A)} \frac{c_B^S(s_A, v_A)}{v_B^S(s_A, v_A)},$$

where the function $M_W^S = M_W^S(s_A, v_A)$ gives the wave Mach number of a post-shock sonic RSW from state (s_A, v_A). From the identity

$$\frac{\partial}{\partial v_A}\left[\frac{v_A}{c(s_A, v_A)}\right]^2 = 2\frac{v_A}{c^2(s_A, v_A)}\left[1 - \frac{v_A}{c(s_A, v_A)}\frac{\partial c(s_A, v_A)}{\partial v_A}\right] = 2v_A\frac{\Gamma(s_A, v_A)}{c^2(s_A, v_A)}$$

the derivative of the function $\widehat{M}_W^S(s_A, v_A)$ is easily obtained as

$$M_W^S \frac{\partial M_W^S}{\partial v_A} = v_A \frac{\Gamma(s_A, v_A)}{c^2(s_A, v_A)}\left[\frac{c_B^S(s_A, v_A)}{v_B^S(s_A, v_A)}\right]^2 + \frac{1}{2}\left[\frac{v_A}{c(s_A, v_A)}\right]^2 \frac{\partial}{\partial v_A}\left[\frac{c_B^S(s_A, v_A)}{v_B^S(s_A, v_A)}\right]^2. \tag{3.4}$$

Since $v > 0$, the sign of the first term of (3.4) is the sign of Γ. From (3.3), the second term of (3.4) is always positive, since the slope of the Rayleigh line increases if the pre-shock state specific volume is increased (see figure 3). Therefore, along a given isentrope, the extrema of the function M_W^S are located within the $\Gamma < 0$ region, where the two terms in (3.4) have opposite sign. Moreover, since the Mach number is unity at A^D and B^D, and since $\partial M_W^S/\partial v_A > 0$ if $\Gamma > 0$, as is the case in the region bounded by the DSL and the $\Gamma = 0$ line, at least one maximum value of the wave Mach number must exist between A^D and B^D.

Figure 5(*a*) reports the wave Mach number along different isentropes crossing the $\Gamma < 0$ region. Along a given isentrope, M_W^S is found to exhibit only one maximum

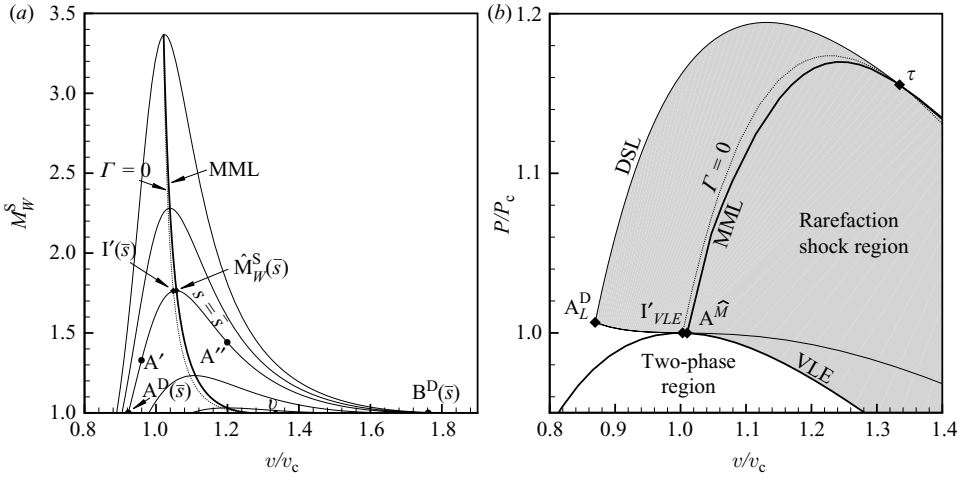

FIGURE 5. (*a*) Wave Mach number along selected isentropes for a van der Waals polytropic fluid with $N = 2000$. The initial states A^D, A' and A'' in figure 2 are also indicated. Along each isentrope, the wave Mach number exhibits only one maximum $\hat{M}_W^S(s)$; the maximum Mach locus (MML) connects these extrema. For a van der Waals polytropic fluid with $N = 2000$ the maximum wave Mach number in the vapour phase is 28.2 (see figure 7). (*b*) The MML in the reduced volume–pressure plane v/v_c–P/P_c. The MML connects point τ, where M_W is one, to point $A^{\hat{M}}$ at the intersection with the VLE line, where M_W is maximum. Note that the MML lies entirely within the $\Gamma < 0$ region.

value, which is located within the $\Gamma < 0$ region. By varying the pre-shock entropy s_A, these extrema describe the maximum Mach locus (MML) depicted in figures 5(*a*) and 5(*b*). Along the MML, the wave Mach number starts from unity at τ and increases for decreasing entropies. Therefore, the maximum wave Mach number for a given fluid is obtained for a post-shock sonic RSW with pre-shock state located at the intersection $A^{\hat{M}}$ of the MML with the VLE curve.

3.3. *Maximum shock strength*

The shock conditions leading to an RSW with maximum strength $\hat{\Pi}$ are now discussed. The shock strength Π is defined as

$$\Pi = \Pi(P_B, P_A, v_A) \equiv \frac{P_B - P_A}{c^2(P_A, v_A)/v_A}, \tag{3.5}$$

and it depends on both a single post-shock thermodynamic variable, e.g. the pressure P_B, and the complete thermodynamic state in A. Note that for an ideal polytropic gas one has $c_A^2 = \gamma P_A v_A$, and therefore the strength of a (classical) shock simply reads $\Pi = [P_B/P_A - 1]/\gamma$; i.e. it depends only on the dimensionless pressure ratio P_B/P_A and on γ. By following the procedure detailed in the previous sections, the maximum strength $\hat{\Pi}$ is computed as

$$\begin{aligned}\hat{\Pi} &= \max_{s_A, v_A, v_B} \frac{v_A}{c^2(s_A, v_A)}\left[P^H(s_A, v_A, v_B) - P(s_A, v_A)\right] \\ &= \max_{s_A, v_A} \frac{v_A}{c^2(s_A, v_A)}\left[P_B^S(s_A, v_A) - P(s_A, v_A)\right],\end{aligned}$$

where in the last expression only the post-shock sonic conditions are considered, since those lead to the largest ΔP for a given pre-shock state A.

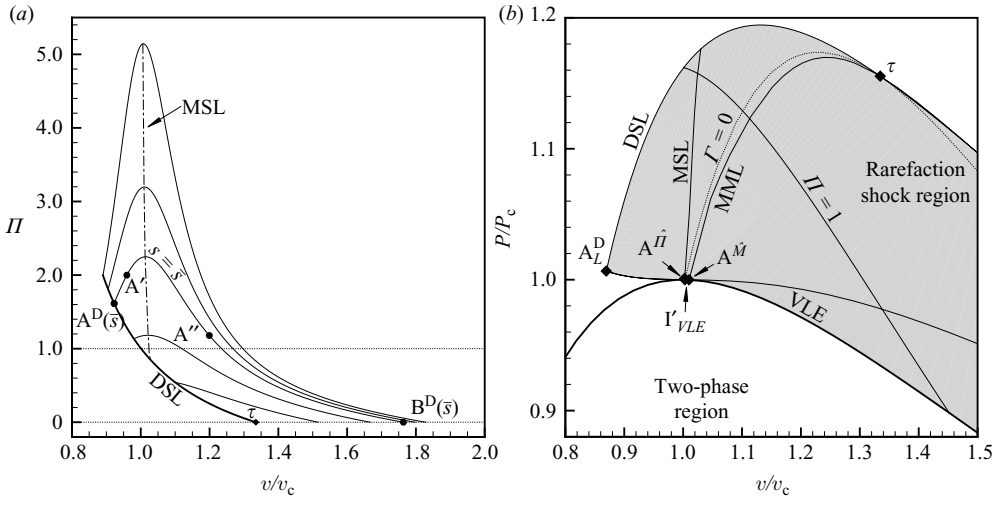

FIGURE 6. (*a*) RSW strength for the post-shock sonic RSW along selected isentropes for a van der Waals fluid with $N = 2000$. Along each isentrope, the post-shock strength is found to exhibit a maximum. All extrema are connected by the MSL. (*b*) The MSL in the reduced volume–pressure v/v_c–P/P_c thermodynamic plane, together with the DSL, the MML, the VLE and the $\Gamma = 0$ curves. The intersection of the MSL and the VLE curve defines the pre-shock state $A^{\widehat{\Pi}}$ from which the RSW with maximum strength $\widehat{\Pi}$ originates.

Similar to what was observed in the problem of the maximization of the wave Mach number (§ 3.2), the strength of post-shock sonic shocks is found to exhibit only one maximum along each isentrope crossing the RSR (see figure 6*a*). It is therefore possible to define a maximum strength locus (MSL) connecting the extrema of each isentrope. The value of Π increases along the MSL from one at τ to a maximum at $A^{\widehat{\Pi}}$, where the MSL intersects the VLE curve (see figure 6*b*).

3.4. *Influence of molecular complexity*

The extension of the RSR and hence the maximum intensity of admissible RSW for a given fluid strongly depend on molecular complexity, as discussed for example by Thompson & Lambrakis (1973), Guardone & Argrow (2005) and Colonna & Guardone (2006). In particular, the higher the molecular complexity, the larger the size – in terms of the pressure and temperature ranges – of the RSR and hence the intensity of admissible RSWs.

Figure 7 reports the minimum value $\Gamma_{\min}$ of the fundamental derivative of gasdynamics in the single-phase vapour, the maximum reduced pressure difference $\widehat{\Delta P}/P_c$ across an RSW, the maximum Mach number $\widehat{M}$ and the maximum RSW strength $\widehat{\Pi}$ for polytropic van der Waals fluids of different molecular complexity. In accordance with the cited references, the value of $\Gamma_{\min}$, which is found at fluid states located on the vapour side of the liquid–vapour coexistence curve, decreases with increasing molecular-complexity parameter N, defined in § 2. Correspondingly, the size of the Γ-negative region and that of the RSR increases with N. Therefore, $\widehat{\Delta P}/P_c$, $\widehat{M}$ and $\widehat{\Pi}$ all increase with N. In figure 7, the reduced pressure difference across the RSW exhibiting the largest wave Mach number $\widehat{M}$ is also depicted, which is significantly different from $\widehat{\Delta P}/P_c$ for all N. Moreover, the maximum reduced pressure difference $\widehat{\Delta P}/P_c$ rapidly saturates to about 1/3 at $N \sim 200$ and slowly

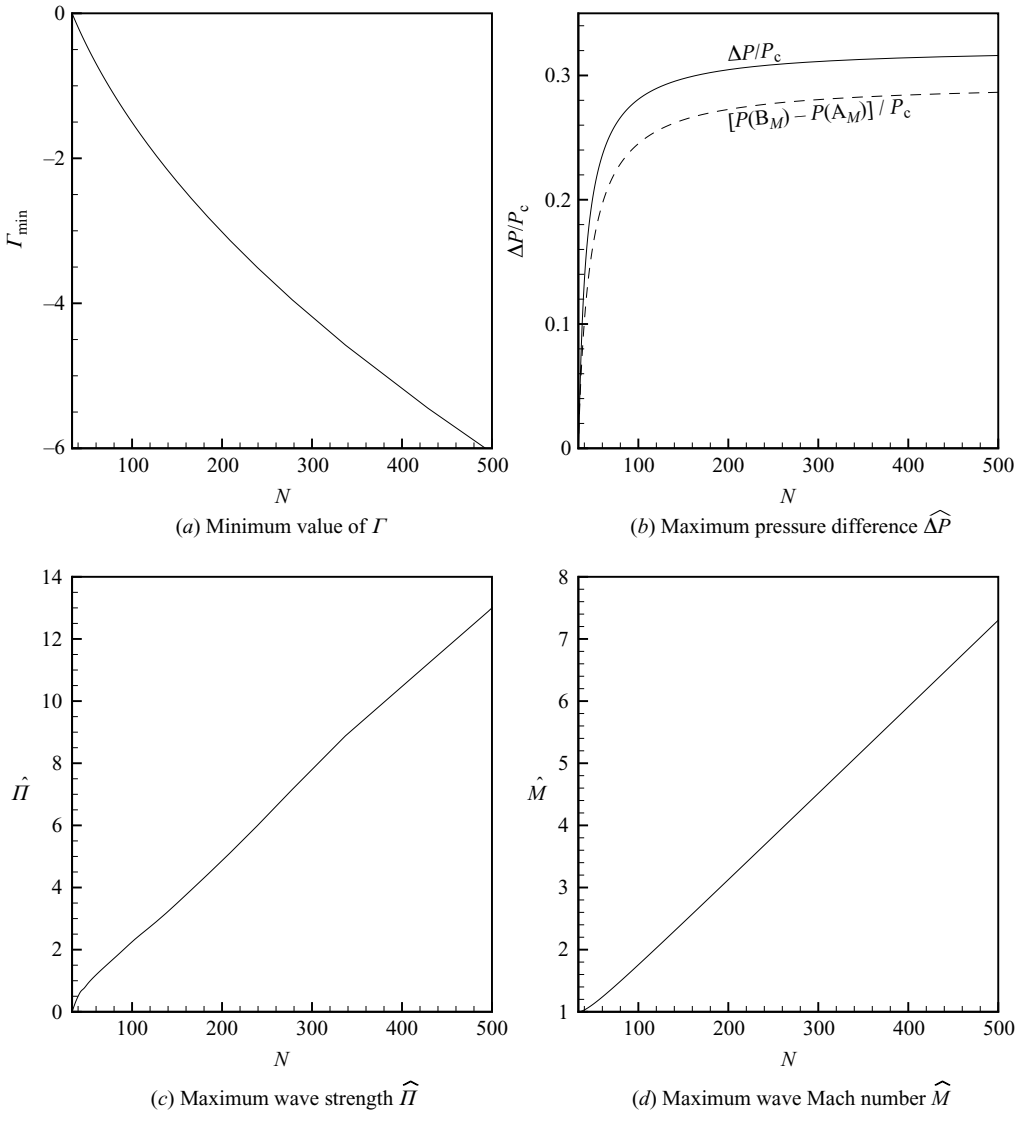

FIGURE 7. Dependence of the maximum intensity of RSWs for fluids with different molecular complexity N, for a polytropic van der Waals gas.

increases for larger values of N. This is not the case for the maximum Mach number and shock strength, as can be appreciated from figure 7.

To conclude, Zamfirescu *et al.* (2008) noted that the shape of the RSR also depends on the molecular complexity of the fluid. In particular, for $N \lesssim 38.46$, at both intersections of the DSL with the VLE one has $v > v_c$, a situation depicted in figure 8 for a polytropic van der Waals fluid with $N = 20$. In this case, the pre-shock state leading to the RSW with maximum pressure difference is no longer located on the DSL, but instead it lies on the vapour side along the VLE curve. The state leading to the RSW with maximum pressure difference is indicated in figure 8 as $\mathrm{A}^{\widehat{\Delta P}}$, and different from the case depicted in figure 4 for $N = 2000$, it is not coincident with A_L^{D}. Remarkably enough, for $N \lesssim 38.46$ the RSW with maximum pressure difference is

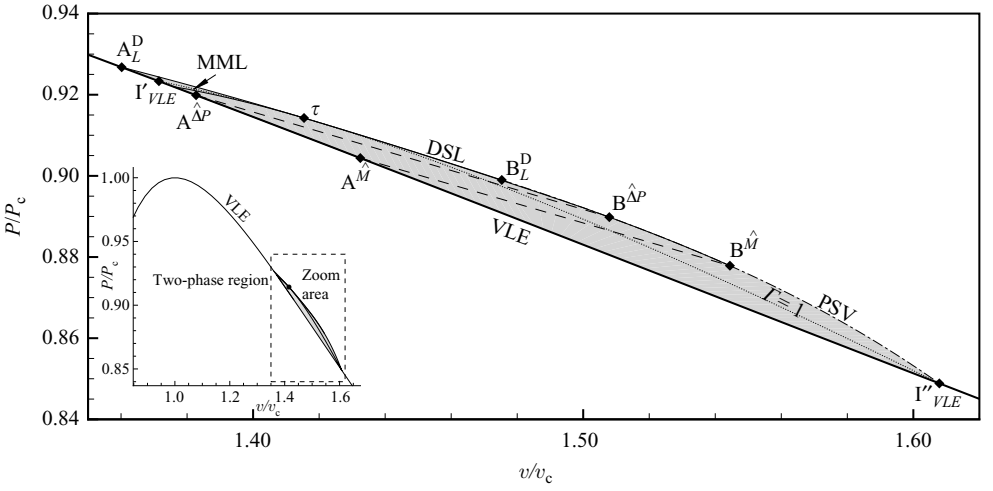

FIGURE 8. RSR for a polytropic van der Waals fluid with $N = 20$. The RSW with the maximum pressure difference and Mach number connects state points $A^{\widehat{\Delta P}}$ $B^{\widehat{\Delta P}}$ and state points $A^{\hat{M}}$ and $B^{\hat{M}}$, respectively.

not a double-sonic shock but a post-shock sonic shock, and it connects the supersonic pre-shock state $A^{\widehat{\Delta P}}$ along the VLE curve to the post-shock sonic state $B^{\widehat{\Delta P}}$ along the PSV curve. Similarly, the RSW with the maximum wave Mach number no longer originates at the intersection of the MML with the VLE curve, but instead it lies on the VLE and, it is indicated in figure 8 as $A^{\hat{M}}$.

The more complex and realistic thermodynamic models considered in the next section all predict a considerably smaller Γ-negative region and hence a smaller RSR, whose shape is though always qualitatively similar to that reported in figure 8.

4. Results for selected siloxanes and perfluorocarbons

The results obtained in the previous section using the simple polytropic van der Waals model are now tested against the more complex non-polytropic Stryjek–Vera–Peng-Robinson (see Stryjek & Vera 1986), Martin–Hou (see Martin & Hou 1955; Martin, Kapoor & De Nevers 1958) and Span–Wagner (see Span & Wagner 2003*a*,*b*) equations of state. These complex equations, whose accuracy in computing the value of Γ has been discussed by Colonna *et al.* (under review), have been applied to the selected linear and cyclic siloxane and perfluorocabons fluids listed in table 1, where relevant thermophysical properties are also reported for the reader's convenience. Additional information on the thermophysical properties of these fluids and their gasdynamic behaviour can be found in Nannan *et al.* (2007) and Colonna *et al.* (2006, 2008*b*) for siloxanes and Lambrakis & Thompson (1972), Cramer (1989, 1991) and Guardone & Argrow (2005) for perfluorocarbons. The minimum value of Γ obtained from the three thermodynamic models is also reported. These complex models include various thermophysical parameters, such as the acentric factor ω, in their functional forms, and therefore the number of active degrees of freedom, N, no longer represents molecular complexity, as discussed by Guardone & Argrow (2005). Therefore, the minimum value of the fundamental derivative in the vapour phase, $\Gamma_{\min}$, which occurs at a state point along the VLE line, is used in the following

Name	M (g mole^{-1})	T_c (K)	P_c (kPa)	T_b (K)	Γ_{min} PRSV	Γ_{min} MH	Γ_{min} SW
D_4	296.618	586.49	1332	448.50	−0.02420	−0.06952	–
D_5	370.773	619.23	1161	484.05	−0.14512	−0.28052	–
D_6	444.924	645.78	961	518.14	−0.22120	−0.38364	−0.23020
MD_4M	459.000	653.20	877	532.72	−0.30407	−0.38457	−0.06900
MD_5M	533.150	671.80	763	599.95	–	−0.44376	–
MD_6M	607.310	688.90	677	584.65	–	−0.49949	–
PP5	462	565.2	1753	415	−0.11041	−0.29834	–
PP9	512	586.6	1682	433	–	−0.43055	–
PP10	574	630.2	1641	467	–	−0.67376	–
PP11	624	650.2	1460	488	–	−0.43891	–
PP24	686	701.2	1530	517	–	−0.10737	–
PP25	774	673.6	1149	533	–	−0.20145	–

TABLE 1. Molecular weight M, critical pressure P_c and critical temperature T_c for selected siloxane and perfluorocarbon fluids; T_b is the boiling temperature at 1 atm; Γ_{min} is minimum value of the fundamental derivative in the vapour phase calculated using different thermodynamic models, namely the Stryjek–Vera–Peng–Robinson cubic equation of state (PRSV) and the Martin–Hou (MH) and Span–Wagner (SW) multi-parameter equations of state. Properties are taken from Stewart, Jacobsen & Penocello (1969), Lambrakis & Thompson (1972), Cramer (1989, 1991), Guardone & Argrow (2005), Nannan *et al.* (2007) and Colonna *et al.* (2006, 2008*b*).

to evaluate the molecular complexity of a given substance. In particular, molecular complexity increases as Γ_{min} decreases, in accordance with figure 7(*a*). Indeed, for a polytropic van der Waals gas, Γ_{min} is shown to be a monotonically decreasing function of N. The minimum value of Γ obtained from the three thermodynamic models is reported in table 1. It is remarkable that the predicted value of Γ, being a derived thermodynamic property, strongly depends on the considered thermodynamic model, as discussed by Thompson & Lambrakis (1973), Guardone & Argrow (2005) and Colonna *et al.* (under review).

Results from the more complex thermodynamic models are listed in table 2, where the maximum pressure difference $\widehat{\Delta P}$, wave Mach number $\widehat{M}_W$ and wave strength $\widehat{\Pi}$ are reported, together with the pressure and temperature of the corresponding pre-shock state. Figure 9 shows $\widehat{\Delta P}$, $\widehat{M}_W$ and $\widehat{\Pi}$ plotted against the minimum value Γ_{min} of the fundamental derivative of gasdynamics in the single-phase vapour region. Note that, different from figure 7, molecular complexity increases from left to right. Figure 9 confirms, at least qualitatively, the results obtained in the previous section using the simple van der Waals model (see figure 7). In particular, the maximum wave Mach number and the shock strength are found to monotonically increase with decreasing Γ_{min}, namely for increasing molecular complexity (figures 7*c*, 7*d*, 9*b* and 9*c*). It is worthwhile noticing that the values of $\widehat{M}_W$ and $\widehat{\Pi}$ strongly depend on the considered thermodynamic model. This is believed to be caused by the differences in the computed value of Γ_{min} (see table 1). Indeed, for a given value of Γ_{min}, all models agree fairly well in the computed value of $\widehat{M}_W$ and $\widehat{\Pi}$.

Considering now the maximum pressure drop across an RSW (figure 9*a*), the data appear to be more scattered, whereas the polytropic van der Waals model predicts a monotonic dependence of $\widehat{\Delta P}$ on molecular complexity (see figure 7). Note that, different from the polytropic van der Waals case, in figure 9(*a*) the pressure differences

		Maximum pressure difference			Maximum wave Mach number			Maximum wave strength		
Name	EOS	P_A (kPa)	T_A (K)	$\widehat{\Delta P}$ (kPa)	P_A (kPa)	T_A (K)	$\widehat{M}_W$ (−)	P_A (kPa)	T_A (K)	$\widehat{\Pi}$ (−)
D_4	MH	1268	310.02	1.205	1233	308.05	1.004	1268	310.02	0.376
	PRSV	1215	306.74	0.297	1200	305.89	1.000	1216	306.79	0.079
D_5	MH	1150	345.44	2.395	1123	343.85	1.045	1150	345.44	1.092
	PRSV	1124	343.78	1.334	1087	341.38	1.011	1124	343.78	0.502
D_6	MH	955.9	372.30	2.226	935.7	370.90	1.072	955.9	372.30	1.327
	PRSV	943.8	371.37	1.444	912.7	369.00	1.023	943.8	371.37	0.716
	SW	947.2	371.67	1.570	917.8	369.57	1.026	947.2	371.67	0.768
MD_4M	MH	873.2	379.74	2.051	855.0	378.35	1.076	873.2	379.74	1.472
	PRSV	869.0	379.37	1.564	841.1	377.09	1.039	869.0	379.37	0.917
	SW	837.9	377.13	0.603	809.1	374.90	1.003	837.9	377.13	0.294
MD_5M	MH	760.3	398.43	1.871	746.3	397.25	1.094	760.3	398.43	1.589
	PRSV	623.0	384.91	2.825	736.0	396.17	1.050	623.0	384.91	1.243
MD_6M	MH	674.5	384.91	1.691	663.3	414.51	1.113	674.5	384.91	1.725
PP5	MH	1688	289.38	2.054	1633	287.03	1.009	1688	289.38	0.524
	PRSV	1719	288.96	1.706	1663	286.53	1.007	1719	288.96	0.398
PP9	MH	1652	312.12	2.895	1597	309.70	1.025	1652	312.12	0.882
PP10	MH	1627	356.34	3.431	1585	354.40	1.048	1627	356.34	1.126
PP11	MH	1455	376.73	3.506	1421	374.89	1.084	1455	376.73	1.536
PP24	MH	1522	427.66	3.811	1507	426.80	1.158	1522	427.66	1.881
PP25	MH	1145	400.21	2.791	1121	398.71	1.092	1145	400.21	1.666

TABLE 2. RSW shock waves with maximum pressure drop, maximum wave Mach number and strength for the fluids listed in table 1, according to the PRSV, MH and SW equations of state (EOS). The pre-shock state A is also reported.

have not been reduced using the critical pressure P_c, which assumes a different value for each fluid. However, despite the large dispersion of the results, the trend observed in § 3 is confirmed by the more complex thermodynamic model, namely the maximum pressure difference across an RSW slowly increases with $\Gamma_{\min}$ for $\Gamma_{\min} \gtrsim -0.2$.

If the analysis is limited to the most recently developed thermodynamic model (see Span & Wagner 2003*a*,*b*; Colonna *et al.* 2007, 2008*b*), which is arguably the most reliable, the RSW with maximum wave Mach number is obtained for fluid D_6, for which one has $\widehat{M}_W \simeq 1.026$.

5. Conclusions

The pre- and post-shock conditions leading to an RSW with the maximum pressure difference, wave Mach number and strength have been investigated. The identification of such states is of the utmost importance in experiments aimed at proving the existence of non-classical gasdynamic phenomena in the vapour phase. These results are also of interest in practical applications aiming at making use of molecularly complex fluids operating close to or within the non-classical gasdynamic region such as the organic Rankine cycle turbines.

The pre- and post-shock states leading to rarefaction shocks with maximum intensity have been identified by means of a three-parameter maximization procedure. Further inspection of the properties of the Rankine–Hugoniot curves in the non-classical region allowed further simplification of the maximization problem.

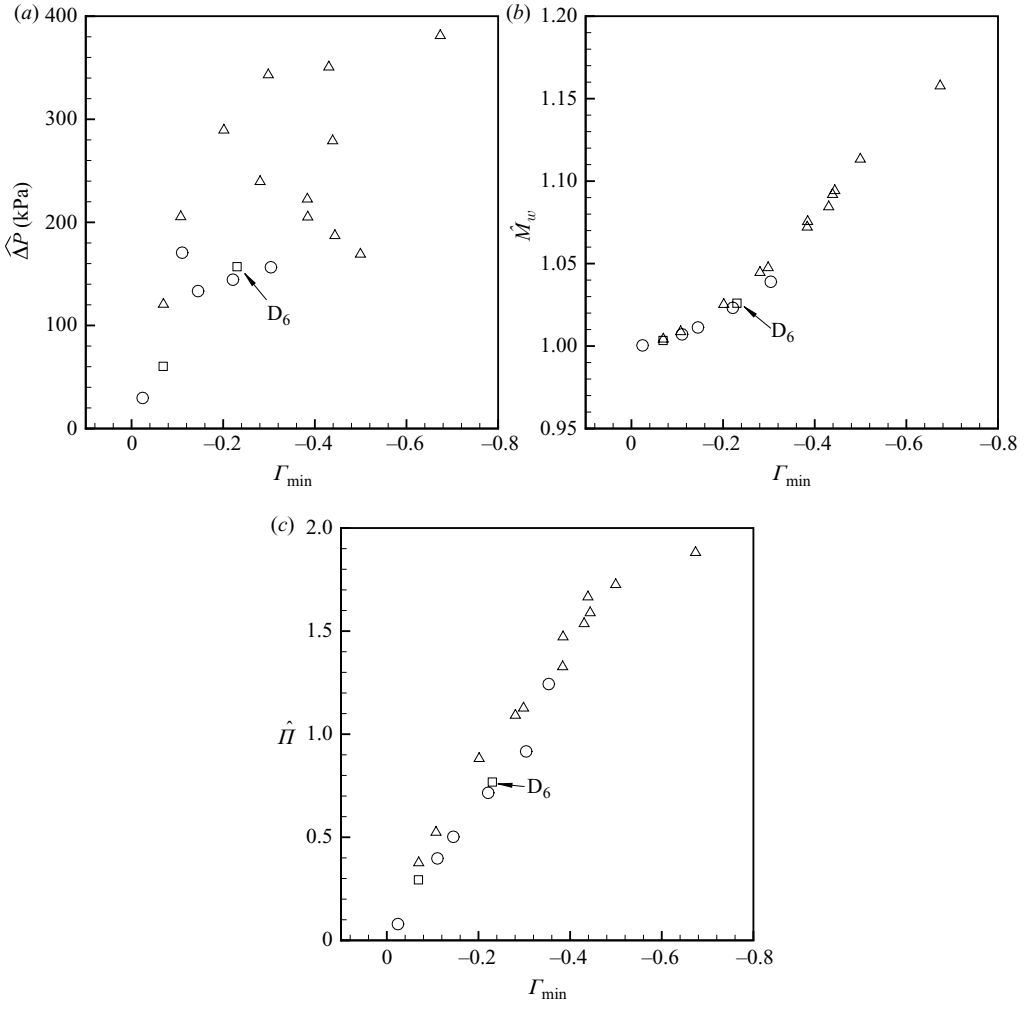

FIGURE 9. Maximum intensity of RSWs, calculated with the Stryjek–Vera–Peng–Robinson (○), Martin–Hou (△) and Span–Wagner (□) equations for the siloxane and perfluorocarbon fluids listed in tables 1. (*a*) Maximum pressure difference across an RSW, (*b*) maximum Mach number for an RSW and (*c*) maximum strength for an RSW.

In a general case, the pre-shock state leading to the maximum pressure difference is located along the DSL of state points that can be connected by a double-sonic shock. The resulting RSW is indeed a double-sonic shock wave. The pre-shock state is found at the intersection of the DSL with the limiting Rankine–Hugoniot curve which is tangent to the VLE curve. Along each isentrope crossing the $\Gamma < 0$ region, the wave Mach number has been found to exhibit only one maximum value. These extrema define a curve in the volume–pressure thermodynamic plane that has been christened the MML. The pre-shock state leading to the maximum wave Mach number is located at the intersection of the MML and the VLE curve. Similarly, the MSL connects the state points along different isentropes from which the RSW with maximum strength can possibly originate. The pre-shock state leading to the strongest shock in the single-phase region is found at the intersection of the MSL and

the VLE curve. Minor modifications to the above procedure are required for fluids with lower molecular complexity.

The simple polytropic van der Waals gas model has been used to determine the dependence of the maximum pressure difference, wave Mach number and strength on the molecular complexity of the fluid. The molecular complexity for this simple model is in a one-to-one correspondence with the number of active degree of freedom of the molecules, including the translational, rotational and vibrational modes. All the indicators of the wave intensity increase with increasing molecular complexity. However, the maximum pressure difference is found to rapidly saturate to a value of about one third of the critical pressure.

These results have been confirmed by the more complex Stryjek–Vera–Peng–Robinson, Martin–Hou and Span–Wagner thermodynamic models. If these equations of state are applied, the maximum value of the pressure difference across an RSW does not depend monotonically on the molecular complexity, which, for complex thermodynamic models, correlates to the minimum value of the fundamental derivative of gasdynamics, Γ, in the single-phase vapour region. According to the multi-parameter Span–Wagner equation of state, the RSW with maximum wave Mach number is obtained for fluid D_6, for which one has $\widehat{M}_W \simeq 1.026$.

The theoretical results herein illustrated have been already employed to design, in collaboration with the Politecnico di Milano, a dense gas Ludwieg tube experiment which is currently under way at the Delft University of Technology. The goal of this experiment is the proof of the existence of non-classical RSWs. Initial fluid states for the experiments will be set with the aim of maximizing the wave Mach number, which are estimated using the theory illustrated in this work. Additional information on the experiment can be found in Colonna *et al.* (2008*a*).

This research has been supported by the Dutch Technology Foundation STW, Applied Science Division of NWO and the Technology Program of the Ministry of Economic Affairs, DSF 6573. The authors acknowledge the contribution of their colleague and friend Ryan Nannan for discussions on thermodynamic models.

REFERENCES

Angelino, G. & Invernizzi, C. 1993 Cyclic methylsiloxanes as working fluids for space power cycles. *Trans. ASME, J. Sol. Energy* **115** (3), 130–137.

Bethe, H. A. 1942 The theory of shock waves for an arbitrary equation of state. *Tech Rep.* 545. Office of Scientific Research and Development.

Borisov, A. A., Borisov, A. A., Kutateladze, S. S. & Nakoryakov, V. E. 1983 Rarefaction shock waves near the critic liquid–vapour point. *J. Fluid Mech.* **126**, 59–73.

Brown, B. P. & Argrow, B. M. 2000 Application of Bethe–Zel'dovich–Thompson fluids in organic rankine cycle engines. *J. Propul. Power* **16** (6), 1118–1124.

Calderazzi, L. & Colonna, P. 1997 Thermal stability of R-134a, R-141b, R-13I1, R-7146, R-125 associated with stainless steel as a containing material. *Intl J. Refrig.* **20** (6), 381–389.

Callen, H. B. 1985 *Thermodynamics and an Introduction to Thermostatistics*, 2nd edn. Wiley.

Colonna, P. 1996 Fluidi di lavoro multi componenti per cicli termodinamici di potenza [Multicomponent working fluids for power cycles]. PhD thesis, Politecnico di Milano, Milan, Italy.

Colonna, P. & Guardone, A. 2006 Molecular interpretation of nonclassical gasdynamics of dense vapours under the van der Waals model. *Phys. Fluids* **18** (5), 056101-1–056101-14.

Colonna, P., Guardone, A. & Nannan, R. 2007 Siloxanes: a new class of candidate Bethe–Zel'dovich–Thompson fluids. *Phys. Fluids* **19** (8), 086102-1–086102-12.

Colonna, P., Guardone, A., Nannan, R. & van der Stelt, T. P. 2009 On the computation of the fundamental derivative of gasdynamics Γ using equations of state. *Fluid Phase Equilib.* In Press, Available on line 30 July 2009, doi:10.1016/j.fluid.2009.07.021.

Colonna, P., Guardone, A., Nannan, R. & Zamfirescu, C. 2008*a* Design of the dense gas flexible asymmetric shock tube. *J. Fluids Engng* **130**, 034501-1–034501-6.

Colonna, P., Nannan, R. & Guardone, A. 2008*b* Multiparameter equations of state for siloxanes: $[(CH_3)_3\text{-Si-}O_{1/2}]_2\text{-}[O\text{-Si-}(CH_3)_2]_{i=1,\ldots,3}$ and $[O\text{-Si-}(CH_3)_2]_6$. *Fluid Phase Equilib.* **263**, 115–130.

Colonna, P., Nannan, R., Guardone, A. & Lemmon, E. W. 2006 Multi-parameter equations of state for selected siloxanes. *Fluid Phase Equilib.* **244**, 193–211.

Colonna, P. & Silva, P. 2003 Dense gas thermodynamic properties of single and multicomponent fluids for fluid dynamics simulations. *ASME J. Fluids Engng* **125**, 414–427.

Cramer, M. S. 1989 Negative nonlinearity in selected fluorocarbons. *Phys. Fluids* **1** (11), 1894–1897.

Cramer, M. S. 1991 Nonclassical dynamics of classical gases. In *Nonlinear Waves in Real Fluids* (ed. A. Kluwick), pp. 91–145. Springer.

Cramer, M. S. & Park, S. 1999 On the suppression of shock-induced separation in Bethe–Zel'dovich–Thompson fluids. *J. Fluid Mech.* **393**, 1–21.

Cramer, M. S. & Sen, R. 1986 Shock formation in fluids having embedded regions of negative nonlinearity. *Phys. Fluids* **29**, 2181–2191.

Cramer, M. S. & Sen, R. 1990 Mixed nonlinearity and double shocks in superfluid helium. *J. Fluid Mech.* **221**, 233–261.

Fergason, S. H., Guardone, A. & Argrow, B. M. 2003 Construction and validation of a dense gas shock tube. *J. Thermophys. Heat Transfer* **17** (3), 326–333.

Fergason, S. H., Ho, T. L., Argrow, B. M. & Emanuel, G. 2001 Theory for producing a single-phase rarefaction shock wave in a shock tube. *J. Fluid Mech.* **445**, 37–54.

Guardone, A. 2007 Three-dimensional shock tube flows of dense gases. *J. Fluid Mech.* **583**, 423–442.

Guardone, A. & Argrow, B. M. 2005 Nonclassical gasdynamic region of selected fluorocarbons. *Phys. Fluids* **17** (11), 116102–1–17.

Hayes, W. 1960 The basic theory of gasdynamic discontinuities. In *Fundamentals of Gasdynamics: High Speed Aerodynamics and Jet Propulsion* (ed. H. W. Emmons), vol. 3, pp. 416–481. Princeton University Press.

Ivanov, A. G. & Novikov, S. A. 1961 Rarefaction shock waves in iron and steel. *Zh. Eksp. Teoret. Fiz.* **40** (6), 1880–1882.

Kluwick, A. 2001 Theory of shock waves. Rarefaction shocks. In *Handbook of Shockwaves* (ed. G. Ben-Dor, O. Igra, T. Elperin & A. Lifshitz), vol. 1, chapter 3.4, pp. 339–411. Academic.

Kutateladze, S. S., Nakoryakov, V. E. & Borisov, A. A. 1987 Rarefaction waves in liquid and gas-liquid media. *Annu. Rev. Fluid Mech.* **19**, 577–600.

Lambrakis, K. C. & Thompson, P. A. 1972 Existence of real fluids with a negative fundamental derivative. *Phys. Fluids* **15** (5), 933–935.

Lax, P. D. 1957 Hyperbolic systems of conservation laws. Part II. *Comm. Pure Appl. Math.* **10**, 537–566. doi:10.1002/cpa.3160100406

Liu, T. P. 1975 The Riemann problem for general systems of conservation laws. *J. Diff. Equations* **18**, 218–234.

Martin, J. J. & Hou, Y. 1955 Development of an equation of state for gases. *AIChE J.* **1** (2), 142–151.

Martin, J. J., Kapoor, R. M. & De Nevers, N. 1958 An improved equation of state. *AIChE J.* **5** (2), 159–160.

Menikoff, R. & Plohr, B. J. 1989 The Riemann problem for fluid flow of real material. *Rev. Mod. Phys.* **61** (1), 75–130.

Nannan, R., Colonna, P., Tracy, C. M., Rowley, R. L. & Hurly, J. J. 2007 Ideal-gas heat capacities of dimethylsiloxanes from speed-of-sound measurements and ab initio calculations. *Fluid Phase Equilib.* **257** (1), 102–113.

Nannan, R. N. 2009 Advancements in nonclassical gasdynamics. PhD thesis, Delft University of Technology, Delft, The Netherlands.

Oleinik, O. 1959 Uniqueness and stability of the generalized solution of the Cauchy problem for a quasilinear equation. *Uspehi Mat. Nauk.* **14**, 165–170.

Smoller, J. 1983 *Shock Waves and Reaction–Diffusion Equations*. Springer.

Span, R. & Wagner, W. 2003*a* Equations of state for technical applications. Part I. Simultaneously optimized functional forms for nonpolar and polar fluids. *Intl J. Thermophys.* **24** (1), 1–39.

Span, R. & Wagner, W. 2003*b* Equations of state for technical applications. Part II. Results for nonpolar fluids. *Intl J. Thermophys.* **24** (1), 41–109.

Stewart, R. B., Jacobsen, R. T. & Penocello, S. G. 1969 *ASHRAE Thermodynamic Properties of Refrigerants*. ASHRAE.

Stryjek, R. & Vera, J. H. 1986 PRSV: an improved Peng–Robinson equation of state for pure compounds and mixtures. *Can. J. Chem. Engng* **64**, 323–333.

Thompson, P. A. 1971 A fundamental derivative in gasdynamics. *Phys. Fluids* **14** (9), 1843–1849.

Thompson, P. A. 1988 *Compressilbe Fluid Dynamics*. McGraw-Hill.

Thompson, P. A. 1991 Liquid–vapour adiabatic phase changes and related phenomena. In *Nonlinear Waves in Real Fluids* (ed. A. Kluwick), pp. 147–213. Springer.

Thompson, P. A., Carofano, G. A. & Kim, Y. 1986 Shock waves and phase changes in a large heat capacity fluid emerging from a tube. *J. Fluid Mech.* **166**, 57–96.

Thompson, P. A., Chaves, H., Meier, G. E. A., Kim, Y. G. & Speckmann, H. D. 1987 Wave splitting in a fluid of large heat capacity. *J. Fluid Mech.* **185**, 385–414.

Thompson, P. A. & Lambrakis, K. C. 1973 Negative shock waves. *J. Fluid Mech.* **60**, 187–208.

van der Waals, J. D. 1873 Over de continuïteit van den gas – en vloeistoftoestand [On the continuity of the gas and liquid state]. PhD thesis, Leiden University, Leiden, The Netherlands.

Weyl, H. 1949 Shock waves in arbitrary fluids. *Comm. Pure Appl. Math.* **2**, 102–122.

Zamfirescu, C., Guardone, A. & Colonna, P. 2008 Admissibility region for rarefaction shock waves in dense gases. *J. Fluid Mech.* **599**, 363–381.

Zel'dovich, Y. B. 1946 On the possibility of rarefaction shock waves. *Zh. Eksp. Teoret. Fiz.* **4**, 363–364.